

Dr. Nicolas Le Novère
Editor

2
3

Computational Systems Neurobiology

4
5

UNCORRECTED PROOF

Editor 6
Nicolas Le Novère
Wellcome Trust Genome Campus
European Bioinformatics Institute
EMBL-Outstation-Hinxton
Wellcome-Trust Genome Campus
Hinxton, Cambridge
United Kingdom 7
8

ISBN 978-94-007-3857-7 ISBN 978-94-007-3858-4 (eBook)
DOI 10.1007/978-94-007-3858-4 9
Springer Dordrecht Heidelberg London New York

Library of Congress Control Number: xxxxxxxxxx 10

© Springer Science+Business Media Dordrecht 2012 11

This work is subject to copyright. All rights are reserved by the Publisher, whether the whole or part of the material is concerned, specifically the rights of translation, reprinting, reuse of illustrations, recitation, broadcasting, reproduction on microfilms or in any other physical way, and transmission or information storage and retrieval, electronic adaptation, computer software, or by similar or dissimilar methodology now known or hereafter developed. Exempted from this legal reservation are brief excerpts in connection with reviews or scholarly analysis or material supplied specifically for the purpose of being entered and executed on a computer system, for exclusive use by the purchaser of the work. Duplication of this publication or parts thereof is permitted only under the provisions of the Copyright Law of the Publishers location, in its current version, and permission for use must always be obtained from Springer. Permissions for use may be obtained through RightsLink at the Copyright Clearance Center. Violations are liable to prosecution under the respective Copyright Law. 12
13
14
15
16
17
18
19
20
21
22

The use of general descriptive names, registered names, trademarks, service marks, etc. in this publication does not imply, even in the absence of a specific statement, that such names are exempt from the relevant protective laws and regulations and therefore free for general use. While the advice and information in this book are believed to be true and accurate at the date of publication, neither the authors nor the editors nor the publisher can accept any legal responsibility for any errors or omissions that may be made. The publisher makes no warranty, express or implied, with respect to the material contained herein. 23
24
25
26
27
28

Printed on acid-free paper 29

Springer is part of Springer Science+Business Media (www.springer.com) 30

Foreword

1

It is now well accepted that the concept “one gene-one protein-one function” is largely inadequate to understand life. The corresponding biomedical concept “one gene-one phenotype-one disease” is even more problematic. Many diseases are multifactorial, but moreover, mono- or multifactorial, the expression of almost all dysfunctions depends on the person and its environment. Systems Biology is a discipline born after second world war, based on control theory, in particular cybernetics, and systems theory. Systems Biology can be briefly summarised as the study of the emerging properties of a biological system taking into account all the necessary constituents, their relationships and their temporal variation. It relies on integration between experimental observations of different types and computer simulations of the system’s dynamics. The field stayed relatively ignored during a few decades, mainly restricted to quantitative analysis of metabolic systems in 1970s and 1980s, as well as signalling pathways a bit later. The conjunction of increased computer power and high-throughput quantitative data production allowed the subject to become in a decade (1998–2008) the new paradigm in biology. A systems approach could allow significant progresses in the understanding and treatment of numerous pathologies, and in particular in the field of neurological diseases. One of the consequences of the rise of Systems Biology has been a change of attitude towards mathematical models in biology (and the corresponding computer simulations). Not only those models are now used routinely, but their size has increased and they are often accompanied by an important semantic layer allowing to link them to biological knowledge. Therefore it became crucial to be able to exchange and reuse those models. This need has triggered the creation of an entire domain of research and development, the “computational systems biology”, comprising research groups, companies, scientific events, etc., an evolution reminiscing of the bioinformatics explosion at the beginning of 1990s.

Among the key concepts in systems biology are quantitative modelling and simulations of biological systems’ behaviour, the necessity of integrate processes at different scales and the emergence at the system level of behaviours unpredictable on the basis of the behaviours of isolated components. Neurosciences occupy a unique position on the three accounts. Since the work of Alan Hodgkin and

Andrew Huxley half a century ago, modelling is a recognised component of research in the domain. Quantitatively describing a cellular behaviour emerging from the interaction between two different molecular components, a potassium and a sodium channel, the work of Hodgkin-Huxley can be seen as the beginning of computational systems biology. Moreover, this modelling activity is frequently pursued together with experimental work. Realistic models are developed at all scales, molecular (signalling pathways), cellular (electrophysiology, growth and differentiation), multicellular (neural networks) and tissular (cerebral electric activity). Synaptic plasticity, neuroadaptation, memory, cognition or consciousness are all emerging phenomena. Neurosciences are therefore the domain by excellence where systems biology concepts can be applied.

Computational studies of neuronal systems, or computational systems neurobiology, require descriptions spanning 12 orders of magnitude in space and 24 orders of magnitude in time. Accordingly, the methods employed are extremely diverse and focus on a subset of the scale considered. When a newcomer enters the field, whether students entering Ph.D. studies or experienced researchers reorienting, the choice of reference books is overwhelming. When I started my group at the EMBLEBI, I used to buy for each student the “yellow book”, “Computational Cell Biology”, by Fall et al. As the research activities of my group expanded, I progressively added other volumes, until the reading list was sufficient to populate half a shelf above each desk. Each book targeting a given audience, its content was highly technical and challenging. I dreamt of a book that I could buy for any of my students, whatever the envisioned Ph.D. topic was. This book would introduce the many different types of computational studies of neuronal systems and would aim to be an entry point for the more specific textbooks of the field, which would be chosen by each student based on their project. Since I could not find any, I decided to contact my colleagues and friends and built it. You have the result in your hands.

The first part of the book deals with molecular systems biology. Functional genomics is presented through examples of transcriptomics and proteomics studies of neurobiological interest. Quantitative modelling of biochemical systems is presented in homogeneous compartments and using spatial descriptions. The second part presents the various approaches to model single neuron physiology. The following part is naturally devoted to neuronal networks. The penultimate division is focused on the development of neurons and neuronal systems. The book closes on a series of methodological chapters. A significant freedom was granted to the authors, and the chapters are of very variable lengths and technical levels. The order is chosen so that one could start from the first chapter and read through until the end. However, each chapter is an independent entity, and you are welcome to read in the order you fancy.

Contents

1	Functional Genomics and Molecular Networks Gene Expression Regulations in Complex Diseases: Down Syndrome as a Case Study	1	2
	Marie-Claude Potier and Isabelle Rivals		3
2	Reconstructing Models from Proteomics Data	23	6
	Lysimachos Zografos, Andrew J. Pocklington, and J. Douglas Armstrong		7
3	Using Chemical Kinetics to Model Neuronal Signalling Pathways ...	81	9
	Lukas Endler, Melanie I. Stefan, Stuart J. Edelstein, and Nicolas Le Novère		10
4	Breakdown of Mass-Action Laws in Biochemical Computation	119	12
	Fidel Santamaria, Gabriela Antunes, and Erik De Schutter		13
5	Spatial Organization and Diffusion in Neuronal Signaling	133	14
	Sherry-Ann Brown, Raquell M. Holmes, and Leslie M. Loew		15
6	The Performance (and Limits) of Simple Neuron Models: Generalizations of the Leaky Integrate-and-Fire Model	163	16
	Richard Naud and Wulfram Gerstner		17
7	Multi-compartmental Models of Neurons	193	19
	Upinder S. Bhalla		20
8	Noise in Neurons and Other Constraints	227	21
	A. Aldo Faisal		22
9	Methodological Issues in Modelling at Multiple Levels of Description	257	23
	Kevin Gurney and Mark Humphries		24
			25

10	Virtues, Pitfalls, and Methodology of Neuronal Network Modeling and Simulations on Supercomputers	26	27
	Anders Lansner and Markus Diesmann		28
11	Co-operative Populations of Neurons: Mean Field Models of Mesoscopic Brain Activity	29	30
	David T.J. Liley, Brett L. Foster, and Ingo Bojak		31
12	Cellular Spacing: Analysis and Modelling of Retinal Mosaics	363	32
	Stephen J. Eglén		33
13	Measuring and Modeling Morphology: How Dendrites Take Shape	34	35
	Todd A. Gillette and Giorgio A. Ascoli		36
14	Axonal Growth and Targeting	427	37
	Duncan Mortimer, Hugh D. Simpson, and Geoffrey J. Goodhill		38 39
15	Encoding Neuronal Models in SBML	457	40
	Sarah M. Keating and Nicolas Le Novère		41
16	NeuroML	487	42
	Padraig Gleeson, Volker Steuber, R. Angus Silver, and Sharon Crook		43 44
17	XPPAUT	517	45
	Bard Ermentrout		46
18	NEST by Example: An Introduction to the Neural Simulation Tool NEST	47	48
	Marc-Oliver Gewaltig, Abigail Morrison, and Hans Ekkehard Plesser		49 50

UNCORRECTED PROOF

Chapter 3

Using Chemical Kinetics to Model Neuronal Signalling Pathways

Lukas Endler, Melanie I. Stefan, Stuart J. Edelstein, and Nicolas Le Novère

Abstract Understanding the physical principles and mechanisms underlying biochemical reactions allows us to create mechanistic mathematical models of complex biological processes, such as those occurring during neuronal signal transduction. In this chapter we introduce basic concepts of chemical and enzyme kinetics, and reaction thermodynamics. Furthermore, we show how the temporal evolution of a reaction system can be described by ordinary differential equations that can be numerically solved on a computer. Finally we give a short overview of different approaches to modelling cooperative binding to, and allosteric control of, receptors and ion channels.

The transduction of neuronal signals and their effects on the behaviours and phenotypes of neurons involve many biochemical entities that interact, diffuse and transform, with different intensities and on different timescales. To understand those biological processes, dynamical and quantitative descriptions are necessary. However, a mere reproduction of experimental observations by non-mechanistic models often is not sufficient, as many experimental results represent averages over time. Furthermore, as the observables are emerging from complex biological systems, in general their behaviour can only be predicted and fully understood by considering the underlying reactions and biophysical processes.

Numerical simulations of models founded in chemical kinetics have been used successfully to describe neuronal signalling for a few decades. Early models concentrated on a single given entity, such as the models of acetylcholine receptors at the neuromuscular junction by Land et al. (1981). Later, models of complex pathways were designed that made full use of the wealth of data accumulated in the field of molecular neurobiology (Bhalla and Iyengar 1999).

L. Endler • M.I. Stefan • S.J. Edelstein • N.L. Novère (✉)
EMBL-EBI, Hinxton, UK
e-mail: lukas.endler@gmx.at; melanie.stefan@cantab.net; stuart.edelstein@unige.ch;
lenov@ebi.ac.uk

In this chapter we introduce basic concepts of chemical and enzyme kinetics, and show how the temporal evolution of a reaction system can be described by ordinary differential equations. Finally we give an overview of different approaches to model cooperative binding to, and allosteric control of, receptors and ion channels.

3.1 Introduction to Chemical Kinetics

A neuron, as any living cell, is built up as a series of compartments of various dimensions. The post-synaptic membrane is an example of a bi-dimensional compartment surrounding the cytosol of the dendritic spine, which is itself a tri-dimensional compartment. Microtubules are examples of uni-dimensional compartments. These compartments can be considered both as containers—we can count the number of instances of a certain type of entity present in, or attached to, a compartment—and as diffusional landscapes—the movements of the entities within the compartment depend on its properties. Within the compartments, the entities can move and react with each other. The object of chemical kinetics is to study the temporal evolution of the positions and quantities of the entities contained in a compartment, sometimes called a reactor.

In this chapter, we will not deal with the displacement of the chemical entities within a compartment. This question will be treated in Chap. 5. We will assume that an entity-pool, that is a set of entities that are indistinguishable as far as the model is concerned, is distributed homogeneously within the compartment. This hypothesis is known as the *well-stirred approximation* (Fig. 3.1). This approximation is based on the assumption that there is no diffusional anisotropy in the compartment, i.e. the molecules move randomly in any dimension.

3.1.1 Chemical Reactions

A chemical reaction is the transformation of one set of substances called reactants into another set called products. At a microscopic scale, such a transformation is in general reversible, although there are many cases in which the reverse reaction is of negligible importance compared to the forward one. In all cases, a reversible reaction can be split into forward and reverse reactions. For a given reaction, reactants generally combine in discrete and fixed ratios to form products. These ratios indicate the amount of each substance involved in the reaction. The amounts consumed or produced in one reaction event are called the stoichiometric coefficients or numbers, ν_X , and are positive for products, and negative for reactants. If a substance is neither consumed or produced by a reaction, its stoichiometric coefficient is 0. Equation 3.1 depicts a general reaction, in which A and B are reactants combining to form the product P. ν_A would be $-a$, $\nu_B = -b$ and $\nu_P = p$. The list $\{-a, -b, p\}$ is also called the stoichiometry of the reaction.



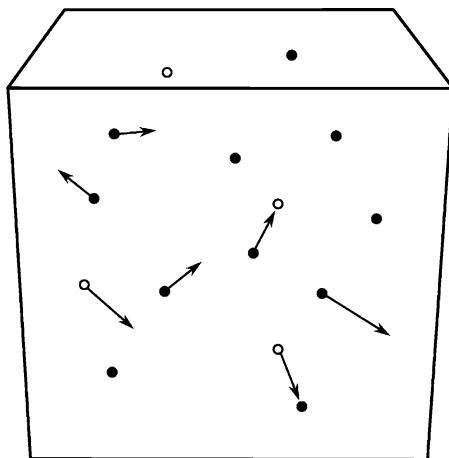


Fig. 3.1 Representation of a well-stirred container with two types of entities, represented by empty and filled circles. The arrows represent the direction and speed of their movements

$$P(\text{reaction } \bullet) = P(\text{find } \bullet) \times P(\bullet \text{ reacts})$$

$$P(\text{reaction } \bullet + \bullet) = P(\text{find } \bullet) \times P(\text{find another } \bullet) \times P(\bullet \text{ reacts with } \bullet)$$

$$P(\text{reaction } \bullet + \circ) = P(\text{find } \bullet) \times P(\text{find } \circ) \times P(\bullet \text{ reacts with } \circ)$$

$$\text{and } P(\text{find } \bullet) \propto \frac{n(\bullet)}{V} = [\bullet]$$

where V is the volume of the container

In many cases in biology only an overall transformation consisting of many sequential reactions is experimentally observable. In the finest grained form these reactions are also known as elementary reactions. An elementary reaction is defined as a minimal irreversible reaction with no stable intermediary products. The lumped stoichiometric coefficients of the overall reaction consist of the sums of the stoichiometric coefficients for each reactant over all elementary reactions.

Chemical kinetics is concerned with the velocity of such transformations, the rates with which substances are consumed and produced. As the rate of change for a reagent depends on its stoichiometric coefficients, it can be different for individual substances. Therefore it is convenient to define the reaction rate, v , as the rate of change of a substance divided by its stoichiometric coefficient. This effectively represents the number of reaction events taking place per unit of time and unit of compartment size.

$$v = \frac{1}{-a} \frac{d[A]}{dt} = \frac{1}{-b} \frac{d[B]}{dt} = \frac{1}{p} \frac{d[P]}{dt}$$

Therefore, we can compute the change of each substance as the product of the reaction rate and its stoichiometric coefficient for this reaction. 79
80

$$\frac{d[A]}{dt} = -a \times v,$$

$$\frac{d[B]}{dt} = -b \times v,$$

$$\frac{d[P]}{dt} = p \times v$$

Reaction rates depend on many factors, and can effectively take any form for the purpose of modelling. In the following subsections, we will describe the simple cases where the reaction rates depend solely on the concentrations of the reacting substances. 81
82
83
84

3.1.2 Mass-Action Kinetics 85

For a chemical reaction to take place, the participants have to collide, or come into close vicinity of each other. The probability of such collisions depends, among other parameters, on the local density of the reactants, and hence, in well stirred environments, on their concentrations.¹ This relationship was first described by Guldberg and Waage in the second half of the nineteenth century in a series of articles on the dynamical nature of the chemical equilibrium (Waage and Guldberg 1864). They assumed that at equilibrium both the forward and backward reaction forces or velocities were equal, and that these velocities were proportional to the concentrations of the reactants to the power of their stoichiometric coefficients. The relationship of reaction velocities and concentrations is called the law “Law of Mass-Action”, and rate expressions equivalent to the ones employed in their articles are sometimes referred to as “Mass-Action Kinetics”.² 86
87
88
89
90
91
92
93
94
95
96
97

The rates of simple unidirectional chemical reactions are usually proportional to the product of the concentrations of the reactants to the power of constant exponents, called *partial reaction orders* or n_X . The sum of all partial orders is called the *order* 98
99
100

¹Under non-ideal conditions, as found in biology, activities instead of concentrations should actually be used both for describing rate equations and equilibria. As this is not common practise in biological modelling, we do not distinguish between activities and concentrations in the following. It should be noted, though, that activities can differ significantly from concentrations in cellular environments.

²The term *mass-action* stems from the proportionality of the so called reaction “force” to the mass of a substance in a fixed volume, which is proportional to the molar concentration of a substance.

n of a reaction, and the proportionality factor is called the *rate constant* k . For example, for the reaction described in Eq. 3.1 assuming mass action kinetics the reaction rate appears as follows:

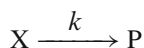
$$v = k \times [A]^{n_A} \times [B]^{n_B}$$

The reaction has an order of $n = n_A + n_B$. In general, the order of elementary reactions is equal to the number of molecules interacting, also known as the *molecularity*. A *unimolecular* reaction $A \rightarrow P$ for example would have an order of one, a *bimolecular* reaction, such as $2A \rightarrow P$ or $A + B \rightarrow P$ would be a second order reaction etc. However, this equivalence is not always true, and anisotropy or crowding of the reaction environments may affect the motion of molecules, resulting in different, and sometimes non-integral, reaction orders.

While mass-action kinetics are only strictly valid for elementary reactions, they are widely and successfully applied in various fields of mathematical modelling in biology. Especially for large and vaguely defined reaction networks, as found in signal transduction, mass action kinetics are commonly employed as a very general initial approach. Most often, the partial orders are taken to be identical to the stoichiometric coefficients. The rate constants can either be calculated from separately measured equilibrium constants and characteristic times, or computationally fitted to reproduce experimental results.

3.1.2.1 Zeroth Order Reactions

Reactions of order zero have a reaction rate that does not depend on any reactant. Zeroth order reactions can be used for instance to represent constant creations from boundary condition reactants, such as:



where X represent a set of source reactants that are not depleted by the reaction. The reaction rate is then equal to:

$$v = k \times [X]^0 = k$$

in which k is the rate constant, and has the units of a concentration per time. The solution describing the evolution of P is of course a monotonic increase:

$$[P](t) = [P_0] + k t$$

3.1.2.2 First Order Reactions

In general unimolecular reactions are modelled using first order mechanisms. In irreversible first order reactions, the reaction rate linearly depends on the concentration

of the reactant. Many decay processes show such kinetics, for example, radioactive decay, dissociation of complexes, or denaturation of proteins. For a simple reaction:



the following rate law applies:

$$v = k \times [A]$$

in which k is the first order rate constant, and has the units of a reciprocal time, $[1/time]$. If this is the only reaction affecting the concentration of A in a system, the change of $[A]$ equals the negative reaction rate. Similarly, the change of $[P]$ equals the reaction rate.

$$\frac{d[A]}{dt} = -v = -k[A]$$

$$\frac{d[P]}{dt} = v = +k[A]$$

The first equation above can be easily rearranged and analytically solved, assuming an initial concentration $[A_0]$ at time $t = 0$. Furthermore, since $[P]_t + [A]_t = [P_0] + [A_0]$:

$$[A]_t = [A_0] \times e^{-kt}$$

$$[P]_t = [P_0] + [A_0] \times (1 - e^{-kt})$$

The rate constant in first order kinetics is directly related to some characteristic times of substances, which are often readily available. For example the average life time of the reactant, τ , and the time it takes for its concentration to halve, the half-life $t_{\frac{1}{2}}$, can be derived as (see Fig. 3.2):

$$\tau = \frac{1}{k}$$

$$t_{\frac{1}{2}} = \frac{\ln 2}{k}$$

3.1.2.3 Second Order Reactions

Second order reactions are often used to model bimolecular reactions, either between different types of molecules or between two instances of the same molecules. Examples are complex formation and dimerisation reactions. For a simple reaction:



the following rate law applies:

$$v = k \times [A] \times [B]$$

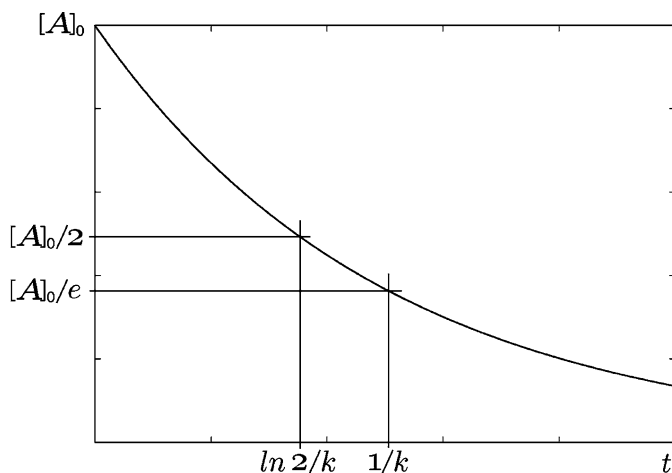


Fig. 3.2 Decay of a reactant A, that is consumed by a first order reaction with a constant k from an initial concentration of $[A_0]$. The average lifetime of a given molecule of A is given by $1/k$. $[A]$ tends toward 0 while $[P]$ tends towards $[A_0] + [P_0]$

in which k is the second order rate constant, and has the unit of $[1/(time \times$ 155
concentration)]. The change of $[P]$ with time is described by the following 156
differential equation: 157

$$\frac{d[P]}{dt} = v = k \times [A] \times [B]$$

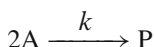
Integration of the above expression using the initial concentrations $[A_0]$, $[B_0]$ and 158
 $[P_0]$ leads to a hyperbolic time dependency: 159

$$[P](t) = [P_0] + [A_0][B_0] \frac{e^{-kt[B_0]} - e^{-kt[A_0]}}{[A_0]e^{-kt[B_0]} - [B_0]e^{-kt[A_0]}}$$

Different from first order reactions, the characteristic times in second order 160
reactions are not independent of the initial conditions, but depend on both the rate 161
constant and the initial concentrations of the reactants. The half life of the limiting 162
reactant, that is B in the case that $[A_0] \geq [B_0]$, is given by the following expression: 163

$$t_{\frac{1}{2}} = \frac{\ln \left(1 + \frac{[A_0] - [B_0]}{[A_0]} \right)}{([A_0] - [B_0])k}$$

A special case of bimolecular reaction, in which two reactant molecules of the 164
same type react to form the product, occurs quite commonly in biology, for example 165
in protein dimerisation reactions. For the general reaction: 166



the reaction velocity and the temporal development of [A] and [P] are given by the following equations: 168
169

$$v = k \times [A] \times [A]$$

$$\frac{d[A]}{dt} = -2v = -2k[A]^2$$

$$\frac{d[P]}{dt} = v = k[A]^2$$

Again, these differential equations can be integrated and, assuming the initial concentrations to be [A₀] and [P₀], resulting time courses for [A] and [P] are described by the following hyperbolic functions: 170
171
172

$$[A](t) = \frac{[A_0]}{2k[A_0]t + 1}$$

$$[P](t) = [P_0] + \frac{2[A_0]kt}{2k[A_0]t + 1}$$

The half life, $t_{\frac{1}{2}}$ of [A] again depends on the initial concentration: 173

$$t_{\frac{1}{2}} = \frac{1}{2k[A_0]}$$

3.1.3 The Thermodynamics of Reactions 174

The field of thermodynamics is concerned with the interconversion of different forms of energy, subsumed mainly under the notions of heat and work, and relates them to changes in observable properties of a system, such as temperature, electrochemical potentials, osmotic pressure, and concentrations of substances. The tools provided by chemical thermodynamics allow us to explore the energetics of a biochemical system and to determine the direction of coupled reactions and processes, such as the transport of ions across a membrane coupled to an electrochemical potential. 175
176
177
178
179
180
181
182

3.1.3.1 Energetics and Equilibrium 183

Central in chemical thermodynamics is the notion of the chemical equilibrium, a state in which all concentrations stay constant over time. While this means that all net reaction fluxes are zero, forward and reverse reactions can still occur, but simply cancel out. Solutions of reacting compounds in a closed environment tend towards a state of equilibrium at which the time evolution of their concentrations stops. In their 184
185
186
187
188

work on the *dynamical* equilibrium Guldberg and Waage found that at equilibrium 189
 a certain ratio of the products and reactants, the so called mass action ratio, Γ , was 190
 constant for specific conditions. This value is called the equilibrium constant, K_{eq} . 191
 For a reversible reaction, Γ is defined as the product of all product concentrations, 192
 divided by the product of the reactants, with each concentration taken to the power 193
 of their stoichiometric coefficients. For the general reaction described in Eq. 3.1 Γ 194
 appears as follows: 195

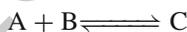
$$\Gamma = \frac{[P]^p}{[A]^a \times [B]^b}$$

and at equilibrium: 196

$$\Gamma_{eq} = K_{eq} = \frac{[P_{eq}]^p}{[A_{eq}]^a \times [B_{eq}]^b} \quad (3.2)$$

The *disequilibrium ratio*, $\rho = \Gamma/K_{eq}$, gives the direction of a reaction. For 197
 $\rho < 1$, a reaction tends towards the products, while for $\rho > 1$ the reverse reaction 198
 rate is greater than that of the forward reaction. 199

The original derivation of K_{eq} by Guldberg and Waage was based on setting 200
 the forward rate of a reaction equal to the backward rate under the assumption of 201
 mass action kinetics. While this approach strictly speaking is only valid for simple 202
 elementary reactions, the derived expression for the equilibrium constant, which 203
 today is also called the *Law of Mass action* (3.2), is still valid under the caveat that 204
 under non-ideal conditions activities, rather than concentrations, have to be used. 205
 For the following reaction with mass action kinetics 206



$$\text{with : } v_f = k_f \times [A] \times [B]$$

$$v_r = k_r \times [C]$$

the following relationship between the rate constants can be derived, by setting the 207
 forward and reverse rate equal: 208

$$v_f = k_f \times [A_{eq}] \times [B_{eq}] = v_r = k_r \times [C_{eq}]$$

$$K_{eq} = \frac{[C_{eq}]}{[A_{eq}][B_{eq}]} = k_f / k_r$$

K_{eq} is related to the Gibb's free energy G , which describes the potential of a 209
 system to perform usable work, or equivalently, to undergo spontaneous change. 210
 The change of G , ΔG , accompanying a process, indicates whether this process 211
 is spontaneous and how much non-expansive work can be obtained during this 212
 change. Non-expansive work can be, for example, the movement of ions to create 213
 an electrochemical potential, fuelling of other non-spontaneous processes, such as 214
 synthesis of ATP, or mechanical work, such as muscle contraction. At equilibrium, 215
 the Gibb's free energy of a system is minimal and $\Delta G = 0$ for all processes. 216

The change of G for a reaction can be defined independent of the reactants' stoichiometries, so that $\Delta_r G$ is the change of G per defined amount of reaction turnover, e.g. 1 mol. These so called reaction Gibbs' free energies can be calculated by subtracting the sum of the reactants' free energies times their stoichiometric coefficients from the products' free energies. For the general reaction described above (3.1) this would mean:

$$\Delta_r G = pG_P - (aG_A + bG_B)$$

In the literature, in general, free energies are given for standard conditions, such as room temperature and substance concentrations of 1 M. These standard reaction free energies, $\Delta_r G^0$, can be used to calculate $\Delta_r G$ for other concentrations of substances, simply by using their mass action ratios Γ . In general, if a reaction has a $\Delta_r G_X$ at a state X with a mass action ratio of Γ_X , then $\Delta_r G_Y$ at state Y with Γ_Y can be written as

$$\Delta_r G_Y = \Delta_r G_X + RT \ln(\Gamma_Y / \Gamma_X)$$

In this R is the universal gas constant, and T stands for the absolute temperature. As at equilibrium the reaction free energy, $\Delta_r G_{eq}$, equals 0 and for standard reaction free energies, $\Delta_r G^0$, the mass action ratio, Γ^0 , is in general equal to 1, the following relation between K_{eq} and $\Delta_r G^0$ can be derived:

$$\begin{aligned} \Delta_r G_{eq} = 0 &= \Delta_r G^0 + RT \ln(K_{eq} / \Gamma^0) \\ \Delta_r G^0 &= -RT \ln K_{eq} \end{aligned}$$

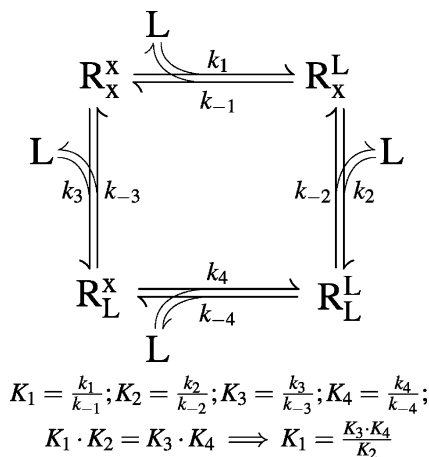
It is also possible to calculate a reaction Gibbs' free energy of a solution from the reaction's mass action ratio Γ and the equilibrium constant:

$$\Delta_r G = RT \ln \frac{\Gamma}{K_{eq}} = RT \ln \rho$$

For coupled reactions, the free energy changes, ΔG , of the individual reactions add up to give the overall change. As reaction free energies are proportional to the logarithm of the equilibrium constants, the overall equilibrium constant can be obtained as the product of the different individual reaction K_{eq} s. In the case of cyclic reaction systems that are not driven by an external energy source, the overall reaction free energy, $\Delta_r G$, is zero, and therefore the product of all equilibrium constants has to equal unity. As the product of all equilibrium constants K_i in a reaction cycle has to equal unity, the same holds true for the product of the ratio of the reverse and the forward rate constants k_{-i} and k_i , respectively. For a cycle of n reactions this leads to the following relationship, also known as detailed balance relation or Wegscheider's cyclicity condition (Heinrich and Schuster 1996):

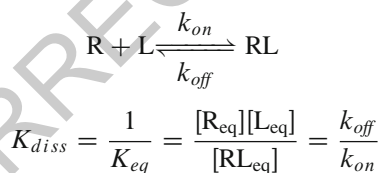
$$\prod_{i=1}^n K_i = 1 = \prod_{i=1}^n \frac{k_{-i}}{k_i}$$

Fig. 3.3 Reaction diagram for binding of a ligand L to two distinct sites on a receptor R . Assuming detailed balance allows us to express one equilibrium constant as a function of the others (After Colquhoun et al. 2004)



Applications of this principle to ions binding to a receptor are shown in Colquhoun et al. (2004). Figure 3.3 illustrates the method for binding of a ligand L to two, distinct binding sites on a receptor R . The detailed balance relation allows us to express one of the equilibria, or one of the rate constants through the other ones.

For binding reactions the inverse of the equilibrium constant, K_{eq} , also known as dissociation constant, K_{diss} is commonly used. In case of a simple complex formation reaction of a receptor R and a ligand L the dissociation constant would be defined as follows:



with k_{on} and k_{off} being the complex association and dissociation rate constants.

3.1.3.2 Transition State and Temperature Dependence of Reaction Rates

Rate constants, in general, show a strong positive temperature dependence, that is, they increase with rising temperatures. This relation was studied in detail in the latter part of the nineteenth century first by Jacobus van't Hoff and Svante Arrhenius. Arrhenius derived an empirical expression for the temperature dependence of the rate constant, k , and postulated a general mechanism underlying this relationship. He assumed that a reaction could only occur if the reacting molecules possessed enough internal energy to overcome a threshold termed activation energy, E_a , and that the proportion of such molecules was given by a Boltzmann distribution.

$$k = Ae^{-E_a/RT}$$

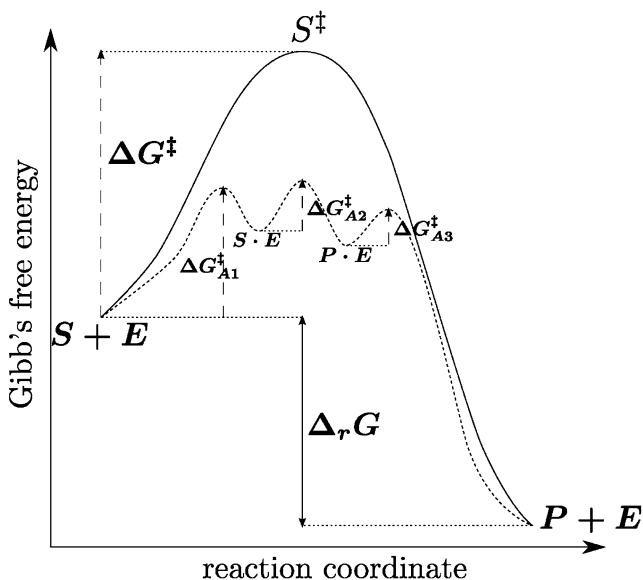


Fig. 3.4 Schematic free energy diagram for the reaction $S \rightarrow P$ without (solid) and with a catalyst (dashed), E . The reaction coordinate is a one-dimensional abstraction of the progress of the reaction. S spontaneously reacts to P via a transition state S^\ddagger . The catalyst E binds S and stabilises the transition state, leading to intermediate steps with a much smaller activation free energy ΔG^\ddagger , thereby accelerating the reaction. The reaction energy $\Delta_r G$ is the same in both cases

In this relation, called Arrhenius equation, A is simply called the *pre-exponential* 265
or *frequency factor*. It can be interpreted as the total frequency of reactant collisions 266
in the correct constellation to react, but not necessarily possessing sufficient energy. 267
A later and more detailed theory is the Transition State Theory, TST, initially 268
pioneered by Henry Eyring and Michael Polanyi in the 1930s. Its basic assumption 269
is that an elementary reaction runs over an unstable activated or transition state 270
(see Fig. 3.4), with a free energy of G^\ddagger . Therefore, to reach the transition state, the 271
participating reactants need at least an activation free energy of $\Delta G^\ddagger = G^\ddagger - G_{gs}$, 272
with G_{gs} being the free energy of the ground state of the reactants. The Eyring 273
equation derived using TST relates k to the free activation energy ΔG^\ddagger and the 274
temperature similar to the Arrhenius equation: 275

$$k = \kappa \frac{k_B T}{h} e^{-\Delta G^\ddagger / RT}$$

Here κ is called the transmission coefficient and indicates the proportion of 276
transition states reacting to give products, k_B is the Boltzmann and h the Planck 277
constant. 278

Catalysts, such as enzymes, work by reducing the free activation energy ΔG^\ddagger . 279
One common possibility for this is to stabilise the transition state. It should always 280
be kept in mind, though, that the reaction free energy, $\Delta_r G$, and with it the 281
equilibrium constant, K_{eq} , is not affected by enzymes. 282

3.1.4 Representing the Evolution of Multi-reaction Systems 283

In the sections above, we only derived expressions describing the temporal evolution 284
of species altered by single reactions. In biological systems, substances are involved 285
in many different processes, leading to complex ordinary differential equation sys- 286
tems, that normally can only be solved numerically and with the help of computers. 287

3.1.4.1 Reconstruction of a System of Ordinary Differential Equations 288

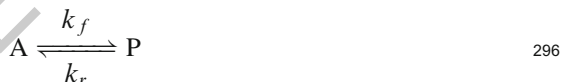
Having carefully designed the elementary processes composing the system, re- 289
constructing the differential equations representing the evolution of the different 290
substances is a systematic and easy procedure. We already saw in Sect. 3.1.2.2 that 291
the reaction: 292



could be modelled by the system: 294

$$\begin{aligned} \frac{d[A]}{dt} &= -1v = -1k[A] \\ \frac{d[P]}{dt} &= 1v = +1k[A] \end{aligned}$$

If the reaction is reversible, such as: 295



then we can consider it as a combination of two irreversible reactions, the rates of 297
which depend on $[A]$ and $[P]$: 298

$$\begin{aligned} v_f &= k_f \times [A] \\ v_r &= k_r \times [P] \end{aligned}$$

The evolution of both substances therefore depends on the forward and reverse 299
reaction rates. A is consumed by the forward reaction and produced by the reverse 300
reaction. It is the other way around for P. 301

$$\begin{aligned} \frac{d[A]}{dt} &= -1v_f + 1v_r = -1k_f[A] + 1k_r[P] \\ \frac{d[P]}{dt} &= +1v_f - 1v_r = +1k_f[A] - 1k_r[P] \end{aligned}$$

To understand how to handle non-unity stoichiometric numbers, consider the following dimerisation:



The forward reaction will be modelled using second-order kinetics, and the rates will therefore be:

$$v_f = k_f \times [A]^2$$

$$v_r = k_r \times [P]$$

As above the evolution of both substances therefore depends on the forward and reverse reaction rates. But this time two molecules of A are consumed by each forward reaction and produced by each reverse reaction. Therefore:

$$\frac{d[A]}{dt} = -2v_f + 2v_r = -2k_f[A]^2 + 2k_r[P]$$

$$\frac{d[P]}{dt} = +1v_f - 1v_r = +1k_f[A]^2 - 1k_r[P]$$

This approach can then be extended, independently of the size of the system considered. An ODE system will contain (at most) one differential equation for each substance. This equation will contain components representing the involvement of the substance in the different reactions of the system. For the substance S_n , involved in a system containing r reactions, the differential equation takes the following form:

$$\frac{d[S_n]}{dt} = \sum_{i=1}^r v_{ni} v_i$$

v_{ni} denotes the stoichiometric coefficient of S_n in reaction i , v_i the rate of this reaction. The resulting ODE system can also be represented in matrix notation, by introducing the stoichiometric matrix, \mathbf{N} , and the reaction rate vector, \mathbf{v} . The stoichiometric matrix, \mathbf{N} , contains a row for each of the n species in the system, and a column for each of the r reactions. Its entries, N_{ij} , are the stoichiometric coefficients, v_{ni} , of substance i in reaction j . \mathbf{v} is a column vector with each element v_i indicating the rate of the i th reaction. Using the above, the change of the concentration vector \mathbf{S} over time is described by:

$$\frac{d[\mathbf{S}]}{dt} = \mathbf{N} \cdot \mathbf{v}$$

3.1.4.2 Numerical Integration of ODE Models

Besides the most elementary systems containing only few well-behaved reactions, we cannot generally solve a system of ordinary differential equations analytically.

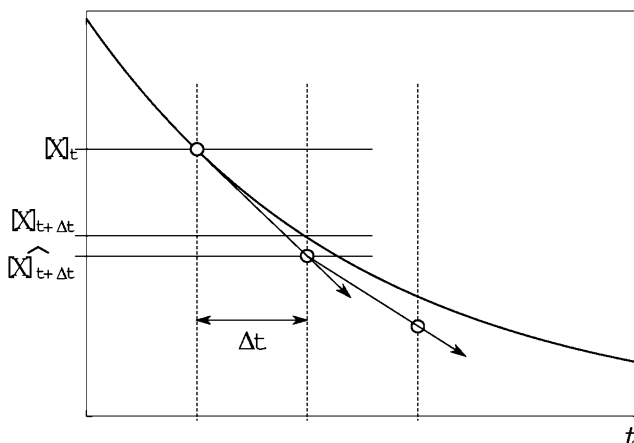


Fig. 3.5 Graphical representation of the forward Euler method to integrate ordinary differential equations. The *thick curve* represents $[X] = f(t)$, and the vectors its derivative. Note the progressive error introduced by the coarse time discretization

We have to resort to numerical integration, a method that goes back to the origin of differential calculus, where we approximate the current values of the variables based on the knowledge we have of their values in the (close) past. Many approximations have been developed. The simplest and easiest to grasp is the forward Euler rule. If we discretize the time, one can make the following approximation:

$$\frac{d[X]}{dt} \approx \frac{\Delta[X]}{\Delta t} = \frac{([X]_{t+\Delta t} - [X]_t)}{\Delta t}$$

We can rearrange the equation above and extract the concentration as follows:

$$[X]_{t+\Delta t} \approx [X]_t + \frac{d[X]}{dt}(t) \times \Delta t$$

We know $d[X]/dt$ as a function of the vector of concentrations, obtained with the method described in Sect. 3.1.4.1, and can therefore compute the difference introduced during one Δt . This procedure is represented in Fig. 3.5. We can see on the figure that a systematic error is introduced by the time discretization. Such an error becomes larger for more complex dynamics, such as non-monotonic behaviours, or systems with fast and slow components. One can address the error by using tiny time steps but at the expense of computational efficacy. Many methods have been developed over the years to address this problem. A good introduction is given in LeMasson and Maex (2001) and a more comprehensive survey of the field by Hairer et al. (1993) and Hairer and Wanner (1996).

Biological modelling tools such as COPASI (Hoops et al. 2006), JDesigner/ 343
 Jarnac (Sauro 2000), E-Cell (Takahashi et al. 2003) or CellDesigner (Funahashi 344
 et al. 2008) have their own in-built numerical ODE solver. They also generate the 345
 system of ODE to be solved automatically, so the user input that is required usually 346
 consists of a list of chemical reactions in some defined format and of the parameters 347
 governing those reactions. 348

3.2 Modelling Biochemical Networks 349

Modelling the biochemical pathways involved in neuronal function does not require 350
 much more than what has been presented in Sect. 3.1. The only complexity we will 351
 introduce in the following sections are slightly more complex expressions for the 352
 reaction rates. 353

3.2.1 Basal Level and Homoeostasis 354

Before modelling the effect of perturbations, such as extracellular signals, it is 355
 important to set up the right basal level for the substances that we will consider in the 356
 model. This basal level is obtained when the processes producing the substance and 357
 the processes consuming it are compensating each other. We then reach a steady- 358
 state, where input and output are equal. To illustrate this, we will build the simplest 359
 system possible that permits to have a steady basal concentration of calcium. The 360
 system is made up of a continuous creation of calcium, for instance due to leaky 361
 channels in the plasma membrane or in the internal stores, modelled as a zeroth 362
 order reaction (see Sect. 3.1.2.1). The calcium is then removed from the system 363
 for instance by pumps or buffers in excess, modelled as a first order reaction (see 364
 Sect. 3.1.2.2). 365



The instantaneous changes of calcium concentration then result from the combi- 367
 nation of the two reaction rates (Fig. 3.6). 368

$$\frac{d[Ca^{2+}]}{dt} = k_{in} - k_{out}[Ca^{2+}]$$

The steady-state level is reached when the changes are null, that is $[Ca^{2+}] =$ 369
 k_{in}/k_{out} . If the concentration of calcium is higher than this ratio, the second term 370
 wins and the concentration decreases. In contrast, if the concentration of calcium 371
 is lower than this ratio, the first term wins and the concentration increases. k_{out} 372

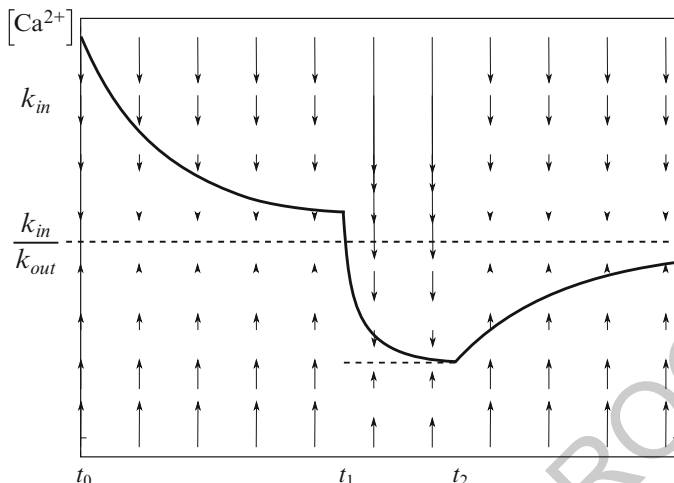


Fig. 3.6 Evolution of calcium concentration over time. Between t_0 and t_1 , the extrusion is stronger than the creation. At t_1 , k_{in} strongly decreases, for instance by a block of leak channels, and the concentration is brought to a lower steady-state value. At t_2 the block is removed. The creation becomes stronger than extrusion, and brings back the concentration to the initial steady-state. Vertical arrows represent the intensity and direction of the reaction's flux for a given concentration of calcium

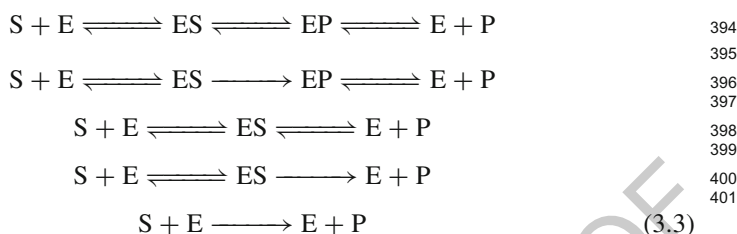
can be estimated from the decay observed after stimulation. k_{in} can therefore be 373
 computed from the steady-state. Changing k_{in} in a discrete manner is a simple way 374
 of modelling the opening or closing of calcium channels. 375

Such a homoeostatic control is extremely simple. More complex schemes can be 376
 designed, with control loops such as negative feed-backs on the creation steps and 377
 positive feedforwards on the extrusion steps. 378

3.2.2 Representing Enzymatic Reactions 379

In order to accelerate chemical reactions and select among different isomers, cells 380
 use enzymes, which are protein-based catalysts. They can increase reaction rates 381
 to a tremendous degree and often are essential to making reactions occur at a 382
 measurable rate. Enzyme catalysed reactions tend to follow complex sequences 383
 of reaction steps, and the exact reaction mechanisms are generally unknown. The 384
 single reaction steps can be contracted into an overall description with lumped 385
 stoichiometries. However, since the detailed reaction mechanisms are most often 386
 unknown, and also parameters for each of these steps are hard to come by, such 387
 reactions can rarely be modelled considering each single step and using mass 388
 action kinetics. Depending on how much detail is known, an enzyme catalysed 389
 reaction can be described on different levels. The reaction equations for a simple 390

conversion of a substrate S to a product P catalysed by an enzyme E, for example, can vary depending on the consideration of intermediate enzyme complexes and reaction reversibility:



Knowledge of the mechanism of an enzymatic reaction can be used to derive compact and simplified expressions fitting the overall kinetics. The alternative is to use generic rate laws that are known to loosely fit wide classes of reaction mechanisms, and to choose the ones that seem most appropriate for the reaction in question. The kinetics of the overall reaction are determined by the reaction mechanisms of the elementary steps, but exact derivations can become quite complex and cumbersome to handle. In general it is safer and more convenient to use approximate expressions in biological modelling, even more so as exact mechanisms are rarely known.

Two assumptions are available to simplify complex enzymatic reaction descriptions. The more general one is the quasi steady state approximation, QSSA. The QSSA considers that some, or all, of the intermediary enzyme substrate complexes tend to a near constant concentration shortly after the reaction starts. The other widely used assumption, called the rapid equilibrium assumption, is that some steps are much faster than the overall reaction, meaning that the participating enzyme forms are virtually at equilibrium and that their concentrations can be expressed using equilibrium constants. This approach is often used to model fast reactant or modulator binding to the enzyme. The application of these techniques depends very much on how much of the reaction mechanism is known. An excellent introduction into enzyme kinetics is given by [Cornish-Bowden \(2004\)](#). For a more exhaustive treatment with detailed derivations of rate laws for a multitude of mechanisms please refer to the standard work by [Segel \(1993\)](#).

3.2.2.1 Henri-Michaelis-Menten Kinetics

At the beginning of the twentieth century, [Henri \(1902\)](#) proposed a reaction scheme and an accompanying expression for describing the rate of sucrose hydrolysis catalysed by invertase. This reaction showed a deviation from normal second-order kinetics and tended to a maximal velocity directly proportional to the enzyme concentration. Making use of the existence of an intermediary substrate-enzyme complex, ES, and assuming that the substrate S and the enzyme E were in a rapid binding equilibrium with the complex, he could derive an expression fitting the

experimental observations. A similar approach was taken and expanded in 1913 432
 by Michaelis and Menten (1913), who proposed the current form of the reaction 433
 rate based on a rapid equilibrium between enzyme and substrate. 434



(k_2 is the catalytic constant, or turnover number, and often called k_{cat} .) 436

A more general derivation, using the QSSA, was proposed by Briggs and 437
 Haldane (1925). The substrate binding and dissociation, as well as the product 438
 formation step, lead to the following expression for the time dependence of [ES]: 439

$$\frac{d[ES]}{dt} = k_1[E][S] - k_{-1}[ES] - k_2[ES]$$

At steady state, the concentration of the intermediate complex, [ES], is constant 440
 hence $d[ES]/dt = 0$. Rearranging this equation and setting $K_M = \frac{k_{-1} + k_2}{k_1}$, we 441
 obtain $[E] = [ES] \times K_M/[S]$. Furthermore, because the concentration of enzyme 442
 is constant, we have $[E] = [E_t] - [ES]$. Equating both, we obtain: 443

$$v = \frac{d[P]}{dt} = k_2[ES] = k_2[E_t] \frac{[S]}{K_M + [S]} \quad (3.4)$$

$k_2 \times [E_t]$ is sometimes called the maximal velocity v_{max} . 444

This rate expression is often used—and abused—when modelling biochemical 445
 processes for which the exact mechanisms are unknown. However, one has to realise 446
 that it only holds true if the concentration of the enzyme-substrate complex stays 447
 constant, which in turns implies that the concentration of substrate is in large excess. 448
 Those conditions are very rarely met in signal transduction systems, resulting in 449
 many artifacts. 450

Plotting the reaction velocity, v , against the substrate concentration, [S], gives 451
 a rectangular hyperbolic curve (see Fig. 3.7). The parameter K_M has the unit of a 452
 concentration and is of central importance in describing the form of the substrate 453
 dependence of the reaction velocity. As can be seen by inserting K_M for [S] in 454
 Eq. 3.4, it denotes the substrate concentration at which the reaction speed is half of 455
 the limiting velocity. If $[S] \ll K_M$, then [S] in the denominator can be disregarded 456
 and the reaction becomes linear with regard to S, showing first order characteristics: 457

$$[S] \ll K_M \Rightarrow v \approx \frac{v_{max}}{K_M} \times [S]$$

On the other extreme, for high substrate concentrations, $[S] \gg K_M$, the reaction 458
 speed becomes virtually independent of [S] and tends toward v_{max} . 459

$$[S] \gg K_M \Rightarrow v \approx v_{max} = k_{cat} \times [E_t]$$

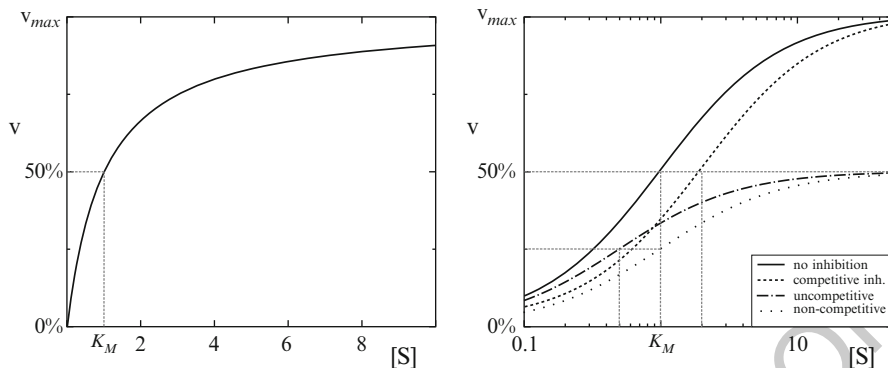


Fig. 3.7 Dependence of the reaction velocity, v , of the irreversible Michaelis Menten equation on the concentration of the substrate, S . The *left graph* shows the uninhibited case. On the *right* various forms of inhibition are shown in a semi-logarithmic plot. The *horizontal dotted lines* indicate the apparent half maximal velocities, the *vertical* ones the apparent K_M s. Competitive inhibition does not alter the maximal velocity, but shifts the K_M to higher values, while non-competitive inhibition simply decreases the apparent v_{max} . The special case of uncompetitive inhibition leads to an apparent increase of substrate affinity of the enzyme, that is a lower K_M , but a reduction of the apparent v_{max} . Mechanistically this is due to the unproductive enzyme-substrate-inhibitor complex ($K_M = 1$; $[I] = 1$; comp., uncom. and non-comp. inhib.: $K_I = 1$)

Most enzyme catalysed reactions show a similar rate behaviour inasmuch as they exhibit first or higher order dependencies on the substrate at lower substrate concentrations and tend to a limiting rate depending only on the enzyme concentration when the reactant concentrations are high.

While the original Michaelis–Menten equation was derived to describe the initial velocity of the enzymatic reaction in absence of product, allowing the reverse reaction to be neglected, the QSSA can also be used to derive a reversible Michaelis–Menten equation describing the most extensive reaction scheme in Eq. 3.3.

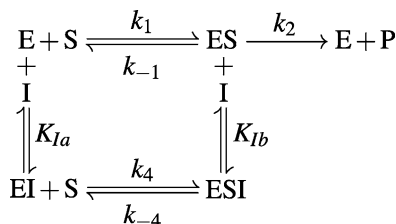
Using the same procedure as above, the following expression for the reaction velocity in dependence of E_T , S and P can be derived:

$$v = \frac{v_{fwd} \frac{[S]}{K_{MS}} - v_{rev} \frac{[P]}{K_{MP}}}{1 + \frac{[S]}{K_{MS}} + \frac{[P]}{K_{MP}}} \quad (3.5)$$

As the net rate of a reversible reaction has to vanish at equilibrium, one of the parameters of Eq. 3.5 can be expressed using the equilibrium constant by setting the numerator of the expression to zero. The so called Haldane relationship connects kinetic and thermodynamic parameters of an enzymatic reaction. While some mechanisms lead to much more complicated expressions, at least one Haldane relationship exists for every reversible reaction.

$$K_{eq} = \frac{v_{fwd} K_{MP}}{v_{rev} K_{MS}} = \frac{k_2 K_{MP}}{k_{-1} K_{MS}}$$

Fig. 3.8 Reversible inhibition of an enzyme E by binding of an inhibitor I . Depending on the values of the dissociation constants K_{Ia} and K_{Ib} , the inhibition can be of competitive, uncompetitive or mixed type



3.2.2.2 Enzyme Regulation

476

An important aspect of enzyme catalysed reactions is the regulation of enzyme activity by effectors or modifications. There are many possible mechanisms for both activation and inhibition of enzymes, often leading to complicated and unwieldy mathematical expressions. Luckily, for modelling purposes crude approximations can be sufficient in many cases.

477
478
479
480
481

Alteration of an enzyme's activity by covalent modifications, such as phosphorylation of cyclin dependent kinases or cleavage in the case of caspases often have to be modelled directly using explicit differential equations for each state. As binding processes are normally much faster, regulation by reversible binding of effectors is more amenable to using rapid equilibrium and steady state assumptions and deriving compact mathematical expressions.

482
483
484
485
486
487

Inhibition can be either *irreversible* or *reversible*, depending on whether the inhibitor disrupts enzyme activity permanently or not. For reversible inhibition, three basic cases can be distinguished, *competitive*, *uncompetitive* and *noncompetitive* inhibition. For these cases, minimal mechanisms can be assumed in combination with the Michaelis Menten scheme as depicted in Fig. 3.8. In this scheme, inhibitor binding is characterised by using the dissociation constants, K_{Ia} and K_{Ib} of the enzyme inhibitor complexes.

488
489
490
491
492
493
494

In *competitive* inhibition, the inhibitor does not alter the limiting rate, but increases the effective Michaelis constant, K_M , the concentration of substrate needed to reach half maximal activity. One possible explanation for this behaviour is that the inhibitor competes with the substrate for the enzyme by binding the same site and blocking it. In the scheme in Fig. 3.8 this corresponds to the inhibitor exclusively binding the free enzyme, $\frac{1}{K_{Ib}} = 0$ and $k_4 = k_{-4} = 0$. Under a quasi steady-state assumption the following dependence of the velocity on the substrate, S , and inhibitor, I , concentrations can be derived:

495
496
497
498
499
500
501
502

$$v = v_{max} \frac{[S]}{K_M \left(1 + \frac{[I]}{K_{Ia}} \right) + [S]}$$

The effect of *uncompetitive* inhibitors on the other hand cannot be counteracted by higher substrate concentrations. They alter both the apparent limiting rate as well as the effective Michaelis constant. In the case of the simple Michaelis Menten mechanism, both v_{max} and K_m are altered by the same factor. This behaviour can

503
504
505
506

be explained by exclusive binding of the inhibitor to the enzyme substrate complex. 507
 In the scheme in Fig. 3.8 this corresponds to $\frac{1}{K_{Ia}} = 0$ and $k_4 = k_{-4} = 0$ and the 508
 following expression can be derived for the velocity: 509

$$v = v_{max} \frac{[S]}{K_M + [S] \left(1 + \frac{[I]}{K_{Ib}}\right)}$$

Noncompetitive inhibition is a rarely occurring case, in which the inhibitor only 510
 alters the apparent limiting velocity. A possible mechanism would be that inhibitor 511
 binds the enzyme independent of the substrate, totally abolishing the enzyme's 512
 activity. In the scheme in Fig. 3.8 this would correspond to $K_I = K_{Ia} = K_{Ib}$ 513
 and $k_4 = k_1, k_{-4} = k_{-1}$ and an expression for the velocity of the form: 514

$$v = v_{max} \frac{[S]}{K_M + [S]} \frac{1}{\left(1 + \frac{[I]}{K_{Ib}}\right)}$$

The more realistic scenario, in which inhibitor binding depends on substrate 515
 binding, is called *mixed* inhibition. With this form of inhibition both the apparent 516
 limiting rate and K_M are altered by the inhibitor. This scenario subsumes all 517
 three other forms of inhibition as special cases with the proper K_{Ia} and K_{Ib} . 518
 An expression for the mixed type mechanism with the scheme in Fig. 3.8 can be 519
 derived by using the steady state assumptions equivalent to those used for derivation 520
 of the irreversible Michaelis–Menten equation (3.4) and considering all possible 521
 enzyme states. This gives an expanded conservation relation for the total enzyme 522
 concentration, $[E_T] = [E] + [ES] + [EI] + [EIS]$. Taking a rapid equilibrium approach 523
 for inhibitor binding, $[EI]$ and $[EIS]$ can be expressed using their dissociation 524
 constants, K_{Ia} and K_{Ib} respectively, and the concentrations of free enzyme and 525
 inhibitor: 526

$$[EI] = \frac{[E] \times [I]}{K_{Ia}} \quad \text{and} \quad [EIS] = \frac{[ES] \times [I]}{K_{Ib}}$$

Proceeding as for Eq. 3.4 the rate law for the simple mixed type inhibition 527
 mechanism in Fig. 3.8 results as: 528

$$v = k_{cat} [E_T] \frac{[S]}{K_M \left(1 + \frac{[I]}{K_{Ia}}\right) + [S] \left(1 + \frac{[I]}{K_{Ib}}\right)}$$

3.2.3 Modelling Simple Transport Processes 529

Compartmentalisation of molecular species and transport across membranes is of 530
 great importance in biological systems, and often needs to be implicitly accounted 531
 for or explicitly included into models. 532

Transport across membranes can either occur passively by simple diffusion, or be coupled to another reaction to actively move molecules against a chemical potential gradient. In the simplest form of passive diffusion, molecules just directly pass through a membrane or an open channel or pore. As the connected compartments in general have differing volumes, the change of concentration of a substance flowing from one compartment to another is not equal in both compartments. Therefore the rate of translocation is commonly described by the flux, j , of a substance, that is the amount of a substance crossing a unit area per time unit. In case of no other influences on the translocation, but simple diffusion, the flux of a substance S into a cell through a membrane follows a variant of Fick's first law:

$$[S_{out}] \rightleftharpoons [S_{in}]$$

$$j_S = p_S ([S_{out}] - [S_{in}])$$

in which $[S_{out}]$ and $[S_{in}]$ are the concentrations of S on the exterior and inside the cell, respectively. p_S denotes the permeability of the membrane for S . The permeability for direct diffusion is proportional to the diffusion coefficient of S and, for pores or channels, to the number of open channels per area.

To derive an expression of the change of concentration of S , it is important to consider that the flux is given as amount per area and time and not as concentration per time. Therefore the volumes of the exterior and the cell have to be included in the differential expressions of concentrations. The overall rate of translocation, v_t , depends on the surface area, A , of the membrane, and the permeability and area can be contracted to a transport rate constant, $k_S = p_S \times A$. For the change of $[S_{out}]$ and $[S_{in}]$, respectively, the following expressions can be derived:

$$\frac{d[S_{out}]}{dt} = -\frac{v_T}{V_{out}} = -\frac{k_S}{V_{out}} ([S_{out}] - [S_{in}])$$

$$\frac{d[S_{in}]}{dt} = \frac{v_T}{V_{in}}$$

with V_{out} and V_{in} being the volumes of the exterior and the cell.

In the case of a molecule that does not simply diffuse through a membrane or pore, but needs to bind a carrier to be translocated from one compartment to the other, the kinetic expressions depend on the exact mechanism of translocation. The simplest case of facilitated, or carrier-mediated, diffusion consists of a carrier with a single binding site, C , which can bind a substance A with equal affinity on each side of the membrane, and flips from one side of the membrane to the other. Using the steady state approach the following expression can be derived for the translocation rate:

$$v_t = \frac{v_{max} ([A_{out}] - [A_{in}])}{K_M + [A_{out}] + [A_{in}] + \frac{K_i [A_{out}][A_{in}]}{K_M}}$$

In this equation v_{max} is the limiting rate of translocation and depends mostly on the amount of carrier. K_M is the concentration of A on one side at half maximal translocation in case of zero concentration on the other side of the membrane, and K_i , called the interactive constant, depends on the relative mobility of the free and loaded carrier (for details see [Kotyk 1967](#)).

3.3 Modelling Cooperative Modulation of Dynamical Processes

Reactions in biological systems are not only regulated by the availability of reactants and catalysts, but also by compounds modulating the activity of channels and enzymes, often without any direct involvement in the specific reactions. Examples are neurotransmitters, such as acetylcholine and gamma-aminobutyric acid, that alter the flow of ions through channels, without direct involvement in the translocation process.

Often, these processes display cooperativity. Intuitively, one can imagine a cooperative scenario as one where the modulating effect of a compound depends on its concentration in a non-linear manner, where *the whole is more (or less) than the sum of its parts*. In this section, we will first introduce useful measures of ligand binding and conformational state, and then examine how cooperativity can be modelled using different frameworks.

3.3.1 Binding of Modulators and Conformational State

The activities of receptors, channels, and enzymes are often regulated by ligands binding to them. One important characteristic of such binding processes is the *fractional occupancy*, \bar{Y} , of the bound compound. It is defined as the number of binding sites occupied by a ligand, divided by the total number of binding sites. For a ligand X binding to a single binding site of a protein P, we can express [PX] and \bar{Y} as follows, using the dissociation constant $K_{diss} = \frac{k_{off}}{k_{on}}$ and the total protein concentration $[P_t] = [P] + [PX]$:

$$\begin{aligned}
 P + X &\xrightleftharpoons[k_{off}]{k_{on}} PX \\
 [PX] &= \frac{[P_t][X]}{K_{diss} + [X]} \\
 \bar{Y} &= \frac{[PX]}{[P_t]} = \frac{[X]}{K_{diss} + [X]}. \tag{3.6}
 \end{aligned}$$

Equation 3.6, also known as the Hill-Langmuir equation, is very similar to the Michaelis–Menten equation. Like [S] in Eq. 3.4, [X] stands for the concentration of *free* ligand, but can be substituted with the total ligand concentration $[X_t] = [X] + [PX]$ in case that $[X_t] \gg [P_T]$.

Often, a protein can exist in various distinct states, only one of which can perform a specific function. Many enzymes, for example, have an inactive state, in which their active site is blocked and an active state, in which this block is relieved. Ion channels can be open and closed. Some proteins exist in two (or more) distinct structural conformations that favour distinct binding partners. We call such a conformation of interest the R state for reasons that will become apparent later in this chapter. Since not all proteins in a population of protein P are necessarily in the same conformation, it is useful to define a *fractional conformational state*, analogous to the previous definition of the *fractional occupancy*. We denote fractional conformational state by \bar{R} and define it as follows:

$$\bar{R} = \frac{[R]}{[P_t]}$$

It is important to note that fractional occupancy and fractional conformational state do not necessarily coincide. Occupancy is usually easier to measure, but the conformational state might be more relevant (and, indeed, sufficient) in some modelling scenarios. Both ligand binding and conformational change can display cooperative behaviour.

In the case of multiple ligand binding sites on a protein, *cooperativity* can arise if the binding of a ligand to one site influences binding to the others. If the binding of a ligand increases the affinity to other ligands, the binding is said to exhibit *positive*, if it decreases the affinity, *negative* cooperativity. Effects of ligands binding to a protein on an activity physically separated from their binding sites are called *allosteric*. They often occur in the regulation of channels by ligands that are structurally unrelated to the transported compounds. Depending on the kind of ligands that influence each others' binding, allosteric and cooperative effects are called *homotropic*, if a ligand influences the binding of ligands of the same kind, or *heterotropic*, if it influences the affinity to ligands of a different kind.

3.3.2 The Hill Equation

The first description of cooperative binding to a multi-site protein was developed by Hill (1910). Drawing on observations of oxygen binding to haemoglobin, Hill suggested the following formula for the fractional occupancy \bar{Y} of a protein with several ligand binding sites:

$$\bar{Y} = \frac{\frac{[X]^h}{K_H}}{1 + \frac{[X]^h}{K_H}} = \frac{[X]^h}{K_H + [X]^h}$$

where $[X]$ denotes ligand concentration, K_H is an apparent dissociation constant (with the unit of a concentration to the power of h) and h is the *Hill coefficient*, which need not be an integer. The *Hill coefficient* h indicates the degree of cooperativity, and in general is different from the number of ligand binding sites, n . While n is an upper bound for h , it is not possible to estimate the binding sites from measurements of the Hill coefficient alone. This is exemplified in Hill's original analysis, in which he found exponents ranging from $h = 1.6$ to 3.2 for the binding of oxygen to haemoglobin, while the heterotetrameric protein possesses four binding sites for O_2 . The Hill equation can show positive and negative cooperativity, for exponent values of $h > 1$ and $0 < h < 1$, respectively. In case of $h = 1$ it shows hyperbolic binding behaviour. With increasing exponents, the ligand binding curve becomes more and more sigmoid, with the limit of a step function with a threshold value of $\sqrt[h]{K_H}$. The number $K_h = \sqrt[h]{K_H}$ gives the ligand concentration at which half the binding sites are occupied, or, in purely phenomenological uses, activation or inhibition by the effector is half maximal.

It is important to note that the above formula, known as the *Hill equation* is a purely phenomenological description of Hills observations of oxygen binding to haemoglobin. It does not offer a mechanistic description of the underlying processes. Because it is a purely phenomenological description, however, it can be used to describe the cooperativity of conformational change as a function of ligand concentration just as well as it can be used to describe the cooperativity of ligand binding. It is enough to replace K_H by a phenomenological constant pertaining to conformational change (the physical equivalent of which we need not worry about) and h by an appropriate Hill coefficient that fits the data for conformational change. Note, however, that the Hill framework does not offer a way of relating ligand saturation and conformational change.

Because the Hill framework is not concerned with a mechanistic explanation of cooperative ligand binding, all binding sites are treated as equal and cooperativity itself does not change with ligand saturation. In other words: Cooperativity in the Hill model is solely a property of ligand molecules, rather than a property of binding sites.

3.3.2.1 Using Hill Functions to Model the Regulation of Biochemical Processes

Hill functions can easily be adapted for use in modelling and to describe interactions with little prior knowledge. Let us assume a channel C transporting a substance S , that is regulated in a nonlinear fashion by a ligand A , for example by direct binding. If the channel is activated with increasing concentrations of A , sometimes this behaviour can be approximated using a Hill function:

$$v_T([C], [A], [S]) = v_{Tmax}([C], [S]) \frac{[A]^h}{K_h^h + [A]^h}$$

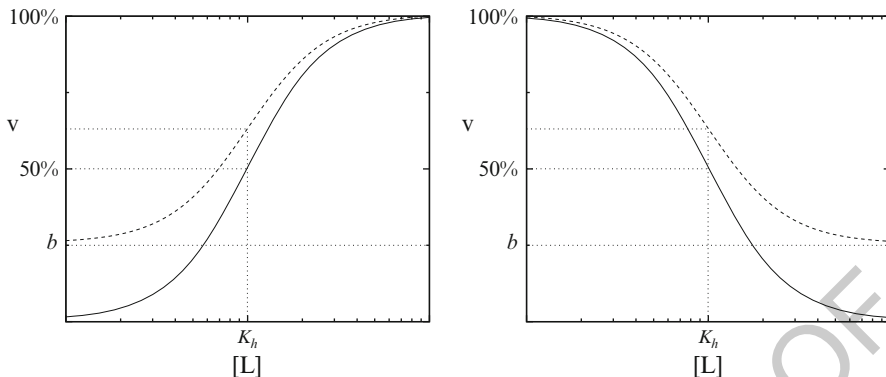


Fig. 3.9 Activation (*left*) and inhibition (*right*) modelled using Hill functions with a Hill exponent, n_h of 2. The concentration of the ligand is shown in units of the concentration of half maximal activation or inhibition, respectively, K_h on a logarithmic scale, the velocity v in percent of the fully activated or uninhibited velocity, v_{max} . The *dashed line* shows cases with a basal rate, v_{bas} , of 25% of v_{max} ($b = \frac{v_{bas}}{v_{max}} = 0.25$)

Here v_T is the actual flux rate of S through the channel C. v_{Tmax} indicates the maximal flux rate at high concentrations of A. K_h and h indicate the ligand concentration of half maximal activation and the Hill coefficient.

An inhibitory effect of a ligand I on the flux through a channel C can often be described using a similar expression:

$$v_T([C], [I], [S]) = v_{Tmax}([C], [S]) \frac{1}{K_h^h + [I]^h}$$

In this equation K_h stands for the concentration at which the ligand I shows half maximal inhibition.

In case of non-essential activation or leaky inhibition, a process still proceeds at a basal rate v_{bas} in absence of the activator or at high concentrations of the inhibitor. This can be accounted for by using the relative basal rate, $b = \frac{v_{bas}}{v_{max}}$:

$$v = v_{max} (b + (1 - b)\gamma([X]))$$

in which $\gamma([X])$ is a function describing the relative activity in dependence of the concentration of the regulating ligand X (Fig. 3.9). In the simplest case for an activating ligand A or an inhibitory ligand I, γ takes the following form:

$$\gamma([A]) = \frac{[A]^h}{K_h^h + [A]^h}$$

$$\gamma([I]) = \frac{1}{K_h^h + [I]^h}$$

The Hill equation is widely used in neuronal modelling, especially for the kinetics of ligand-gated channel. An example containing two different types of activation is given in Borghans et al. (1997) for the Ca^{2+} induced Ca^{2+} release (CICR) via the inositol triphosphate (InsP_3) receptor. Equation 19 in that article describes the release of calcium from a calcium sensitive pool with a flux rate given by:

$$v_{\text{InsP}_3\text{R}} = v_{\text{max}} \frac{[\text{Ca}_p]^2}{K_1^2 + [\text{Ca}_p]^2} \frac{[\text{Ca}_c]^2}{K_2^2 + [\text{Ca}_c]^2}$$

In this equation v_{max} denotes the maximal release rate, and $[\text{Ca}_p]$ and $[\text{Ca}_c]$ the Ca^{2+} concentrations in the pool and the cytoplasm. The release is regulated by the Ca^{2+} concentrations on both sides of the membrane separating the pool and the cytosol, and K_1 and K_2 stand for the threshold concentrations for these activations.

Parthimos et al. (2007) used an even more complex expression for the CICR from the sarcoplasmic reticulum via the InsP_3 receptor. The receptor was modelled to be both activated and inactivated by cytosolic Ca^{2+} , Ca_c , using two Hill functions involving Ca_c . A possible mechanistic explanation for this form would be the existence of independent activation and inhibition sites, with different affinities and degrees of cooperativity for Ca^{2+} . In the flux rate through the InsP_3 receptor

$$v_{\text{InsP}_3\text{R}} = v_{\text{max}} \frac{[\text{Ca}_s]^2}{K_1^2 + [\text{Ca}_s]^2} \frac{[\text{Ca}_c]^4}{K_2^4 + [\text{Ca}_c]^4} \frac{K_3^4}{K_3^4 + [\text{Ca}_c]^4} \quad (3.7)$$

K_2 and K_3 indicate the cytosolic Ca^{2+} concentrations at which activation and inhibition of CICR, respectively, are half maximal. If they are chosen in such a way that $K_2 < K_3$, the flux rate through the receptor reaches a maximum for concentration values between the values of the two constants and vanishes for higher cytosolic Ca^{2+} concentrations (see Fig. 3.10), creating a complex on-off behaviour of the InsP_3 receptor in dependence of the Ca^{2+} concentration.

3.3.3 The Adair-Klotz Framework

Adair (1925) and Klotz (1946) (reviewed in Klotz 2004) further explored the notion of cooperative binding. According to their framework, cooperativity was no longer fixed, but dependent on saturation: Binding of the first ligand molecule would alter the affinity of the protein for the following ligand molecules.

This type of cooperative binding can be elucidated in the simplest case of a protein possessing two identical ligand binding sites. Assuming that the first ligand molecule, X can bind either site of P with a dissociation constant K_1 to give the complex PX and the second molecule with a dissociation constant K_2 to give the complex PX_2 :

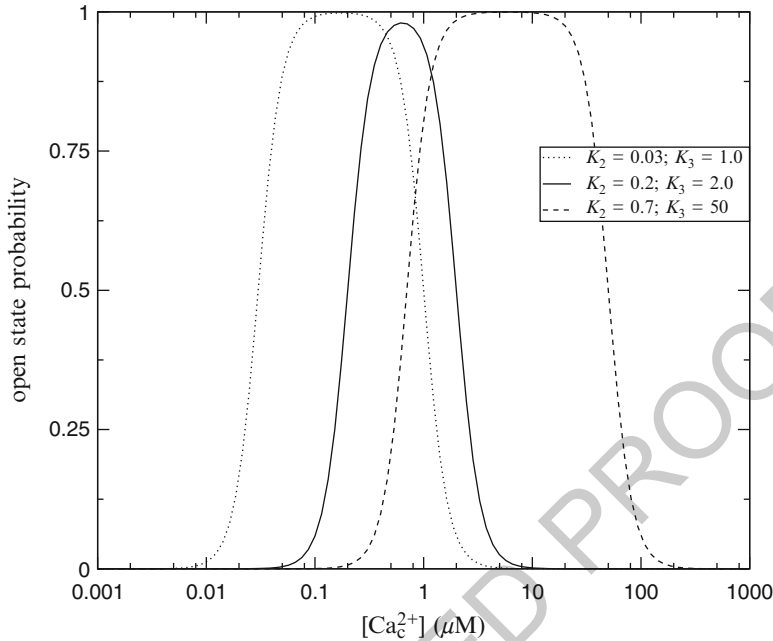
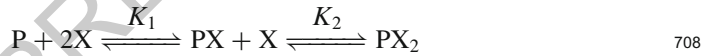


Fig. 3.10 InsP₃ receptor opening probability dependent on cytoplasmic Ca²⁺ after Parthimos et al. (2007) as described in Eq. 3.7. K₂ and K₃ indicate the concentrations of half maximal activation and inhibition, respectively, of the InsP₃ receptor. For both activation and inhibition a Hill factor of 4 was assumed



As the first ligand can choose from two binding sites, a factor 2 has to be included in the expression for [PX]. For the concentrations of the complexes the following relations follow: 709
710
711

$$[PX] = 2 \frac{[P][X]}{K_1} \quad \text{and} \quad [PX_2] = \frac{[P][X]^2}{K_1 K_2}$$

or for the fractional saturation \bar{Y} : 712

$$\bar{Y} = \frac{[PX] + 2[PX_2]}{2([P] + [PX] + [PX_2])} = \frac{\frac{[X]}{K_1} + \frac{[X]^2}{K_1 K_2}}{1 + 2\frac{[X]}{K_1} + \frac{[X]^2}{K_1 K_2}}$$

The two binding affinities, K₁ and K₂ determine the form of cooperativity exhibited by the binding process. If the binding of the ligand to both sites is completely independent, that is K₁ = K₂, the protein exhibits hyperbolic binding. On the other hand, if binding of the first ligand leads to an increased affinity, ie. 713
714
715
716

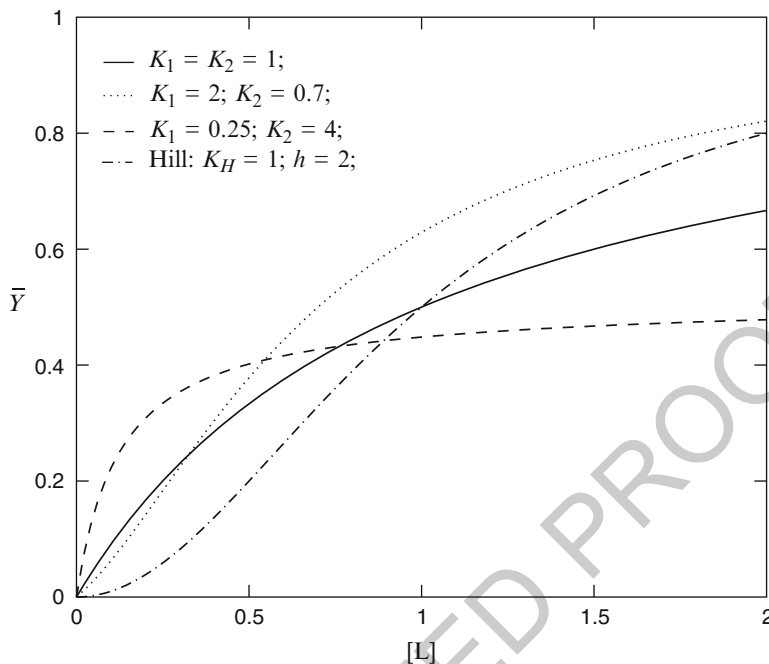


Fig. 3.11 Fractional occupancy \bar{Y} of a protein with two ligand binding sites dependent on the ligand concentration $[X]$. The *solid line* shows the behaviour for independent binding sites ($K_1 = K_2$), the *dotted* for positive ($K_1 < K_2$) and the *dashed* for negative ($K_1 > K_2$) cooperativity between binding sites. Hill type binding with a Hill coefficient of 2 is shown as a boundary case (*dot-dashed line*)

decreased dissociation constant for the second site, $K_1 > K_2$, the protein exhibits 717
 positive cooperativity. In case of negative cooperativity, the binding of the first 718
 ligand decreases the affinity of the second site, $K_1 < K_2$, and the sensitivity of the 719
 protein to the ligand concentration decreases faster than with hyperbolic binding. 720
 Figure 3.11 shows different forms of cooperativity for this binding process. 721

In the case of $K_1 \gg K_2$, the concentration of the intermediary can be neglected 722
 and it can be assumed that the binding occurs in a single step, with both ligands 723
 binding at the same time. In this case, the above equation reduces to a Hill equation 724
 with an appropriate phenomenological dissociation constant K_H . 725

The Adair-Klotz framework gives a sequence of binding constants, exactly as 726
 many as there are binding sites on protein P for ligand X. It is worth noting that 727
 these constants do not relate to individual binding sites. They describe *how many* 728
 binding sites are occupied, rather than *which ones*. In that sense, the reported 729
 dissociation constants are phenomenological. At the same time, they are easily 730
 observable by fitting an Adair-Klotz equation to data on protein saturation as a 731
 function of ligand concentration. They are therefore widely used by experimentalists 732
 to describe measurements of ligand binding in terms of sequential apparent binding 733
 constants. 734

Note that the Adair-Klotz equation cannot be used to describe conformational change, nor is there an easy way to deduce a conformational state from a fractional occupancy. For some applications, this might not be a problem, because conformational information might not be needed, or it might be a good enough approximation to add a simple assignment such as, for instance, equating full ligand saturation with the active state. It needs to be borne in mind, though, that this approximation does not always hold and that some signalling proteins with subtle regulation patterns need to be described using models that account for their conformational state as well as their ligand saturation.

3.3.4 Allosteric Models

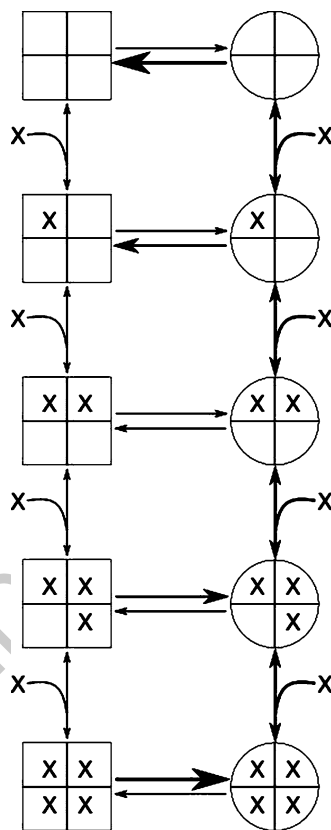
By the middle of the twentieth century, there was an increased interest in models that would not only describe binding curves phenomenologically, but offer an underlying biochemical mechanism. Koshland (1958) and Koshland et al. (1966) offered a tentative biochemical explanation of the mechanism described by Adair (1925) and Klotz (1946) for proteins made of identical subunits with one ligand binding site per subunit. The Koshland, Nemethy and Filmer (KNF) model assumes that each subunit can exist in one of two conformations: active or inactive. Ligand binding to one subunit would induce an immediate conformational change of that subunit from the inactive to the active conformation, a mechanism described as *induced fit*. Cooperativity, according to the KNF model, would arise from interactions between the subunits, the strength of which varies depending on the relative conformations of the subunits involved. This *sequential* model directly links saturation to the conformational state of a subunit. Importantly, it posits that not all subunits of a protein need to be in the same conformational state at the same time.

3.3.4.1 The MWC Model

In contrast, The Monod-Wyman-Changeux (MWC) model of concerted allosteric transitions (Monod et al. 1965) assumes that all subunits in the enzyme undergo conformational change together, a concept known as *concerted* transition. The probability of transition between two conformational states of the proteins, termed the *tense* (T) and the *relaxed* (R) state, depends on the binding of ligands that have different affinities for each of these two states. A schema of an MWC-type protein is shown in Fig. 3.12.

In the absence of a ligand, for instance, the T state prevails, but as more ligand molecules bind, the R state (which has higher affinity for the ligand) becomes more and more populated. Remembering the discussion in Sect. 3.1.3.2, we can describe the situation in terms of free energy: In the absence of ligand, the T state has a lower free energy than the R state and is therefore the preferred state. As more and more ligand binds, however, the R state becomes the energetically favoured conformation (see Fig. 3.13).

Fig. 3.12 Schematic view of an MWC protein with four subunits. The T state is shown as a square, the R state as a circle. In this case, the R state has a higher affinity for the ligand L; ligand binding thus stabilises the R state over the T state



A few new parameters have to be introduced in order to conveniently describe an MWC protein. The allosteric isomerisation constant L describes the equilibrium between both states when no ligand molecule is bound: $L = \frac{[T_0]}{[R_0]}$. If L is very large, most of the protein exists in the tense state in the absence of ligand. If L is small (close to one), the R state is nearly as populated as the T state. While the Adair-Klotz framework traditionally operates with association constants, the MWC framework has traditionally been described using dissociation constants. The ratio of dissociation constants for the R and T states is described by the constant c : $c = \frac{K_d^R}{K_d^T}$. If $c = 1$, both R and T states have the same ligand affinity and the ligand does not affect isomerisation. The value of c also indicates how much the equilibrium between T and R states changes upon ligand binding: the smaller c , the more the equilibrium shifts towards the R state. According to the MWC model (Monod et al. 1965), fractional occupancy is described as follows:

$$\bar{Y} = \frac{\frac{[X]}{K_d^R} \left(1 + \frac{[X]}{K_d^R}\right)^{n-1} + Lc \frac{[X]}{K_d^R} \left(1 + c \frac{[X]}{K_d^R}\right)^{n-1}}{\left(1 + \frac{[X]}{K_d^R}\right)^n + L \left(1 + c \frac{[X]}{K_d^R}\right)^n} \quad (3.8)$$

with K_d^R , L and c as described in the paragraph above.

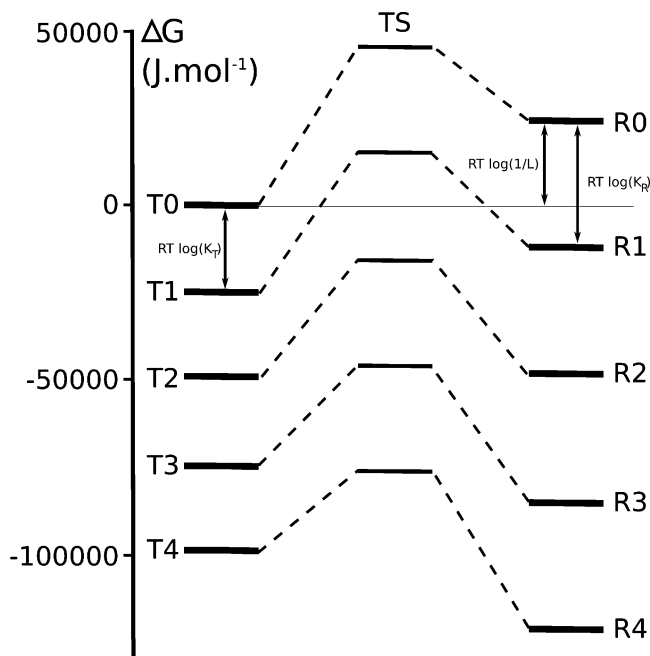


Fig. 3.13 Free energy diagram for an allosteric protein with four binding sites. Energy levels (in J/mol) were computed as in (Edelstein et al. 1996) using an allosteric model of calmodulin (Stefan et al. 2008). Each level of energy represents all the forms carrying the same number of ligand ions. Free energy differences between the T state and the corresponding R state relate to the allosteric isomerisation constant. Between corresponding T and R states, a hypothetical transition state is depicted based on estimates of rate constants. T state is shown on the *left*, R state on the *right* and the transition state in the *middle*

The degree of conformational change is described by the state function \bar{R} , which denotes the fraction of protein present in the R state. As the energy diagram illustrates, \bar{R} increases as more ligand molecules bind. The expression for \bar{R} according to the MWC model (Monod et al. 1965) is:

$$\bar{R} = \frac{\left(1 + \frac{[X]}{K_d^R}\right)^n}{\left(1 + \frac{[X]}{K_d^R}\right)^n + L \left(1 + c \frac{[X]}{K_d^R}\right)^n} \quad (3.9)$$

Thus, the MWC model can express both ligand binding and conformational change as a function of ligand concentration, and the relationship between the two is well defined because both expressions rely on the same set of microscopic parameters. It is important to note that the curves for \bar{Y} and \bar{R} do not overlap (Rubin and Changeux 1966), i. e. fractional saturation is not a direct indicator of conformational state (and hence, of activity). This is illustrated in Fig. 3.14.

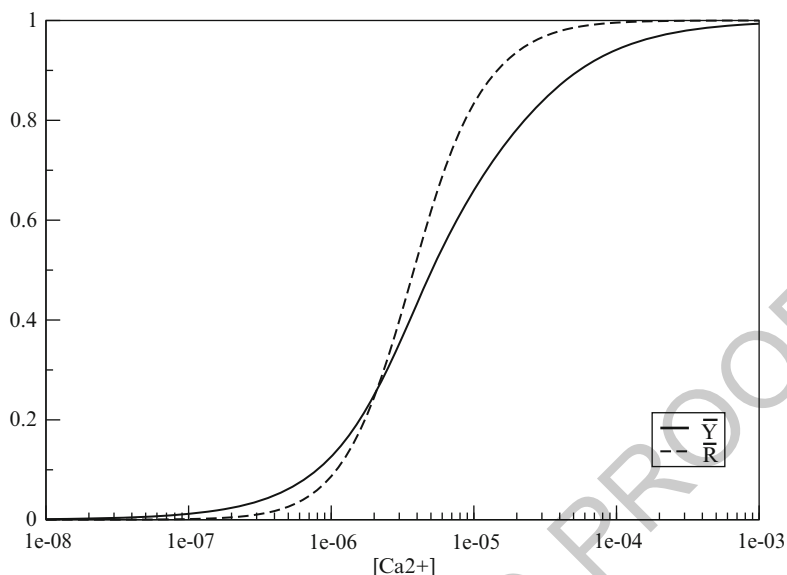


Fig. 3.14 \bar{Y} and \bar{R} for an allosteric protein. Fractional occupancy (\bar{Y}) is shown as a *solid line*; fractional conformational change (\bar{R}) as a *dashed line*. Curves were obtained using a model of calmodulin (Stefan et al. 2008) with a calmodulin concentration of 2×10^{-7} m

Within the MWC model, the function of an allosteric protein can be modulated 798
by an allosteric effector: An effector that binds preferentially to the R state and 799
hence stabilises it is called an allosteric activator, while an effector that prefers the 800
T state is called an allosteric inhibitor (Monod et al. 1965). 801

Generalisation and extensions of the MWC framework have been presented 802
to account for various additional scenarios. Other generalisations of the MWC 803
framework have been presented to account for allosteric proteins with multiple 804
states (Edelstein et al. 1996), for proteins that bind to different types of ligand (Mello 805
and Tu 2005), proteins that bind to several ligands and multiple allosteric activators 806
or inhibitors (Najdi et al. 2006) and proteins with non-identical binding sites for the 807
same ligand (Stefan et al. 2009). 808

The conformational spread model by Duke et al. (2001) is a general allosteric 809
model that encompasses both the KNF model and the MWC model as special cases. 810

3.3.5 Which Framework to Use

811

In theory, the same system can be described using either of the frameworks 812
presented above (and a nice example for data interpreted both using the Adair- 813
Klotz framework and the MWC framework is given in Yonetani et al. 2002), and 814
simpler models arise as special cases from the more complicated ones. However, 815

for the purposes of computational modelling, it is important to bear in mind that the different frameworks describing cooperativity have different scopes, drawbacks and advantages.

The Hill function is quick and easy to implement, features few unknown parameters that can readily be derived by fitting to experimental data, and can be used to describe either ligand binding or activation. On the other hand, it is a purely phenomenological description that will not offer a better mechanistic understanding of the protein-ligand system in question and does not allow for subtle effects such as a change of cooperativity as a function of saturation.

The Adair-Klotz framework is used widely in experimental work on ligand binding to protein. Therefore, dissociation constants found in the literature can often be plugged directly into an Adair-Klotz equation without the need for parameter conversion or estimation. The Adair-Klotz framework is wider in scope than the Hill equation and has more mechanistic relevance in that the association constants are related to real binding events. However, the Adair-Klotz framework itself is strictly limited to ligand binding and disregards conformational change.

The MWC framework accounts for both ligand binding and conformational change and therefore allows for the modelling of rather subtle effects, especially when the two do not coincide. It offers the greatest level of mechanistic detail and is therefore very powerful. However, allosteric parameters such as L and c are rarely found in the experimental literature and are harder to measure than the apparent Adair constants, so the demands on data analysis and parameter estimation are higher.

Note that while all frameworks provide an assignment rule that allows for ligand saturation at equilibrium to be computed from concentration of free ligand, only the Adair-Klotz framework and the MWC framework allow for a separate formulation of forward and reverse reactions, and hence for a representation of kinetic effects.

Also note that the expressions for \bar{Y} in all three frameworks and for \bar{R} in the MWC model only hold if the concentration of free ligand equals that of total ligand, i. e. if ligand supply is unlimited. In biological systems, this is not always the case, which means that the real dose-response curve can differ from the theoretical one. A discussion of this phenomenon, called ligand depletion, is given in [Edelstein et al. \(2010\)](#). An explicit simulation, in which ligand supply is not unlimited and ligand is consumed as the reactions proceed, offers a more realistic approach, although it might be more tedious to implement.

Whatever model is used will depend on a number of factors, including data availability, computational cost, scale of the model, and the biological question under investigation.

3.4 Further Reading

Biophysical chemistry, James P. Allen. This is a complete and concise presentation of the physical and chemical basis of life ([Allen 2008](#)).

- Computational Cell Biology*, Christopher P. Fall, Eric S. Marland, John M. Wagner, 857
 John J. Tyson. Also known as “the yellow book”, this is an excellent introduction 858
 to modelling cellular processes. It contains chapters dedicated to ion channels, 859
 transporters, biochemical oscillations, molecular motors and more (Fall et al. 860
 2002). 861
- Enzyme kinetics*, Irwin H. Segel and *Fundamentals of Enzyme Kinetics*, Athel 862
 Cornish-Bowden. Also known as “the black book” and the “the red book”, these 863
 are the two reference books if one wants to know how to model an enzymatic 864
 reaction, regardless of its complexity. 865
- Solving Ordinary Differential Equations I and II*, Ernst Hairer, Syvert P. Norsett, 866
 Gerhard Wanner. Extensive coverage of the domain of ordinary differential 867
 equations, from Newton and Leibniz to the most advanced techniques using 868
 implicit solvers. 869

References

- Adair GS (1925) The hemoglobin system. IV. The oxygen dissociation curve of hemoglobin. *J Biol Chem* 63:529–545 871
- Allen JP (ed) (2008) *Biophysical chemistry*. Wiley-Blackwell, Oxford 872
- Bhalla U, Iyengar R (1999) Emergent properties of networks of biological signaling pathways. *Science* 283(5400):381–387 873
- Borghans JM, Dupont G, Goldbeter A (1997) Complex intracellular calcium oscillations. A theoretical exploration of possible mechanisms. *Biophys Chem* 66(1):25–41 874
- Briggs GE, Haldane JB (1925) A note on the kinetics of enzyme action. *Biochem J* 19(2):338–339 875
- Colquhoun D, Dowsland KA, Beato M, Plested AJR (2004) How to impose microscopic reversibility in complex reaction mechanisms. *Biophys J* 86(6):3510–3518 876
- Cornish-Bowden A (2004) *Fundamentals of enzyme kinetics*. Portland Press, London 877
- Duke TA, Novère NL, Bray D (2001) Conformational spread in a ring of proteins: a stochastic approach to allostery. *J Mol Biol* 308(3):541–553 878
- Edelstein SJ, Schaad O, Henry E, Bertrand D, Changeux JP (1996) A kinetic mechanism for nicotinic acetylcholine receptors based on multiple allosteric transitions. *Biol Cybern* 75(5):361–379 879
- Edelstein SJ, Stefan MI, Le Novère N (2010) Ligand depletion in vivo modulates the dynamic range and cooperativity of signal transduction. *PLoS One* 5(1):e8449 880
- Fall C, Marland E, Wagner J, Tyson J (eds) (2002) *Computational cell biology*. Springer, New York 881
- Funahashi A, Matsuoka Y, Jouraku A, Morohashi M, Kikuchi N, Kitano H (2008) CellDesigner 3.5: a versatile modeling tool for biochemical networks. *Proc IEEE* 96:1254–1265 882
- Hairer E, Wanner G (1996) *Solving ordinary differential equation II: stiff and differential-algebraic problems*. Springer, Berlin 883
- Hairer E, Nørsett SP, Wanner G (1993) *Solving ordinary differential equations: nonstiff problems*. Springer, Berlin 884
- Heinrich R, Schuster S (1996) *The regulation of cellular systems*. Springer, New York 885
- Henri V (1902) *Theorie generale de l'action de quelques diastases*. *C R Acad Sci. Paris* 135:916–919 886
- Hill AV (1910) The possible effects of the aggregation of the molecules of hæmoglobin on its dissociation curves. *J Physiol* 40:i–vii 887
- Hoops S, Sahle S, Gauges R, Lee C, Pahle J, Simus N, Singhal M, Xu L, Mendes P, Kummer U (2006) COPASI—a complex pathway simulator. *Bioinformatics* 22(24):3067–3074 888

- Klotz IM (1946) The application of the law of mass action to binding by proteins. Interactions with calcium. *Arch Biochem* 9:109–117 903 904
- Klotz IM (2004) Ligand-receptor complexes: origin and development of the concept. *J Biol Chem* 279(1):1–12 905 906
- Koshland DE (1958) Application of a theory of enzyme specificity to protein synthesis. *Proc Natl Acad Sci USA* 44(2):98–104 907 908
- Koshland DJ, Nmethy G, Filmer D (1966) Comparison of experimental binding data and theoretical models in proteins containing subunits. *Biochemistry* 5(1):365–385 909 910
- Kotyk A (1967) Mobility of the free and of the loaded monosaccharide carrier in *saccharomyces cerevisiae*. *Biochim Biophys Acta* 135(1):112–119 911 912
- Land BR, Salpeter EE, Salpeter MM (1981) Kinetic parameters for acetylcholine interaction in intact neuromuscular junction. *Proc Natl Acad Sci USA* 78(11):7200–7204 913 914
- LeMasson G, Maex R (2001) Computational neuroscience. In: De Schutter E (ed) Chapter Introduction to equation solving and parameter fitting, CRC Press, London, pp 1–23 915 916
- Mello BA, Tu Y (2005) An allosteric model for heterogeneous receptor complexes: understanding bacterial chemotaxis responses to multiple stimuli. *Proc Natl Acad Sci USA* 102(48):17354–17359 917 918 919
- Michaelis L, Menten M (1913) Die kinetik der invertinwirkung. *Biochem Z* 49:333–369 920
- Monod J, Wyman J, Changeux JP (1965) On the nature of allosteric transitions: a plausible model. *J Mol Biol* 12:88–118 921 922
- Najdi TS, Yang CR, Shapiro BE, Hatfield GW, Mjolsness ED (2006) Application of a generalized MWC model for the mathematical simulation of metabolic pathways regulated by allosteric enzymes. *J Bioinform Comput Biol* 4(2):335–355 923 924 925
- Parthimos D, Haddock RE, Hill CE, Griffith TM (2007) Dynamics of a three-variable nonlinear model of vasomotion: comparison of theory and experiment. *Biophys J* 93(5):1534–1556 926 927
- Rubin MM, Changeux JP (1966) On the nature of allosteric transitions: implications of non-exclusive ligand binding. *J Mol Biol* 21(2):265–274 928 929
- Sauro H (2000) Jarnac: a system for interactive metabolic analysis. In: Hofmeyr JHS, Rohwer JM, Snoep JL (eds) Animating the cellular map 9th international BioThermoKinetics meeting, chap. 33. Stellenbosch University Press, Stellenbosch, pp 221–228 930 931 932
- Segel IH (ed) (1993) *Enzyme kinetics*. Wiley, New York 933
- Stefan MI, Edelstein SJ, Le Novère N (2008) An allosteric model of calmodulin explains differential activation of PP2B and CaMKII. *Proc Natl Acad Sci USA* 105(31):10768–10773 934 935
- Stefan MI, Edelstein SJ, Le Novère N (2009) Computing phenomenologic Adair-Klotz constants from microscopic MWC parameters. *BMC Syst Biol* 3:68 936 937
- Takahashi K, Ishikawa N, Sadamoto Y, Sasamoto H, Ohta S, Shiozawa A, Miyoshi F, Naito Y, Nakayama Y, Tomita M (2003) E-cell 2: multi-platform E-cell simulation system. *Bioinformatics* 19(13):1727–1729 938 939 940
- Waage P, Guldberg C (1864) Studies concerning affinity. *Forhandlinger: Videnskabs-Selskabet i Christiania* 35 941 942
- Yonetani T, Park SI, Tsuneshige A, Imai K, Kanaori K (2002) Global allosteric model of hemoglobin. Modulation of O₂ affinity, cooperativity, and Bohr effect by heterotropic allosteric effectors. *J Biol Chem* 277(37):34508–34520 943 944 945